PHYSICAL REVIEW B **80**, 201306(R) (2009)

Interplay between superfluidity and magnetic self-trapping of exciton polaritons

I. A. Shelykh,[1] T. C. H. Liew,[2,3] and A. V. Kavokin[4,5]
[1]*Science Institute, University of Iceland, Dunhagi 3, IS-107 Reykjavik, Iceland*
[2]*Centre for Quantum Technologies, National University of Singapore, Singapore 117543, Singapore*
[3]*Ecole Polytecnique Fédérale de Lausanne (EPFL), CH-1015 Lausanne, Switzerland*
[4]*School of Physics & Astronomy, University of Southampton, SO17 1BJ Southampton, United Kingdom*
[5]*Physics Department, University of Rome II, 1, via della Ricerca Scientifica, 00133 Roma, Italy*
(Received 24 July 2009; published 10 November 2009)

In dilute magnetic semiconductor microcavities, exciton polaritons self-localize in real space due to the magnetic polaron effect. The resulting circularly polarized classical condensates can be transformed into superfluids by increasing the temperature and applying an external magnetic field. The interplay between polariton-polariton repulsion and exchange coupling of polaritons with magnetic ions strongly affects the phase diagram for Bose-Einstein condensation of exciton polaritons.

DOI: 10.1103/PhysRevB.80.201306 PACS number(s): 71.36.+c, 42.55.Sa, 42.65.Pc

Features of superfluidity of exciton polaritons in semiconductor microcavities have been recently observed experimentally.[1,2] Theory predicts the formation of linearly polarized polariton superfluids in two-dimensional (2D) microcavities due to a kind of Berezinsky-Kosterlitz-Thouless (BKT) phase transition.[3] A linear polarization minimizes the free energy of the superfluid whose excited states form Bogliubov-like dispersion branches either colinearly or cross linearly polarized with respect to the superfluid. The orientation of the linear polarization is spontaneously chosen by the system in ideal isotropic microcavities or may be pinned to one of the crystal axes in spatially anisotropic systems.[4,5] Furthermore, it has been shown that an external magnetic field gradually transforms the polarization of a polariton superfluid to the elliptic polarization and, above some critical field, to the circular polarization.[6,7]

Here we show that the phase diagram of the superfluid transition in 2D exciton-polariton systems can be strongly modified if a low concentration of magnetic ions is present in the microcavity. The exchange interaction of excitons with the magnetic ions can result in formation of self-trapped, spatially localized, exciton states referred to as exciton-magnetic polarons.[8,9] The critical temperature of magnetic self-trapping is dependent on the exciton effective mass, the exchange constant, and the value and orientation of the external magnetic field applied to the system.[10] It has been suggested by Kavokin *et al.*[11] that the collective exciton-magnetic polaron effect may lead to the formation of condensed circularly polarized exciton states. The magnetic polaron effect is reduced in microcavities in the strong coupling regime where excitons are replaced by exciton polaritons whose effective mass is orders of magnitude lighter. The lighter effective mass results in a lower critical temperature of magnetic self-trapping. On the other hand, the critical temperature for magnetic self-trapping increases as the occupation number of the condensate increases. At low temperatures and high polariton concentrations, the magnetic polaron effect strongly competes with superfluidity, leading to the formation of spatially localized, spin-polarized, classical condensates.

We focus on the transition from classical real space condensation to superfluidity. We show that such a transition takes place at a critical temperature and/or external magnetic field. For realistic $CdTe/Cd_{1-x}Mn_xTe$ microcavities, we expect the critical temperature of this transition to be lower than the BKT critical temperature. The phase diagram is governed by the interplay between the exciton-magnetic ion exchange interaction and the polariton-polariton interaction.

We consider a dilute Bose gas of exciton polaritons in a planar semiconductor microcavity with quantum wells (QW) diluted with magnetic (e.g., Mn^{2+}) ions having spin 5/2. We shall assume that the subsystems of cavity polaritons and magnetic ions can be described by two semiclassical fields interacting with each other. Moreover, we will neglect the finite lifetime of cavity polaritons, assuming that the processes of arrival of polaritons into the condensate (due to an incoherent pump) and radiative decay of condensed polaritons compensate each other. These are the usual simplifying assumptions made while discussing the phase diagrams of exciton-polariton systems.[12,13] The finite lifetime and relaxation dynamics of exciton polaritons can be further taken into account by kinetic modeling,[14] which is beyond the scope of this Rapid Communication.

Being formed usually by heavy-hole excitons, polaritons have two allowed spin projections on the structure growth axis (± 1), corresponding to the right and left circular polarizations of counterpart photons. In the absence of an external magnetic field the "spin-up" and "spin-down" states of noninteracting polaritons, or their linearly polarized superpositions, are degenerate. The situation changes if polariton-polariton scattering is accounted for: the interaction of polaritons in triplet configuration (parallel spin projections on the structure growth axis) is much stronger than that of polaritons in singlet configuration (antiparallel spin projections).[15,16]

Let us start by considering the stationary case. Our goal is to determine a phase diagram in the (B_0,T) plane. Assuming that the external magnetic field is oriented along the structure growth axis (z axis), one has the following expression for the free energy density in the spatially isotropic system:

$$F = -\mu(|\psi_+|^2 + |\psi_-|^2) + \frac{\alpha_1}{2}(|\psi_+|^4 + |\psi_-|^4) + \alpha_2|\psi_+|^2|\psi_-|^2 - \int_{B_0}^{B_{eff}} M_z(B)dB = -\mu n + \frac{\alpha_1+\alpha_2}{4}n^2 + \Delta_\alpha S_z^2 - \tilde{F}, \quad (1)$$

where the second and third terms account for polariton-polariton interactions; the last term accounts for the interaction of the spin of magnetic ions with the external magnetic field and polariton field, $\Delta_\alpha = \alpha_1 - \alpha_2$. α_1 and α_2 denote the constants of interaction between polaritons in triplet and singlet configurations, respectively,[17] $\psi_\pm$ are the right and left circularly polarized polariton fields, $n=|\psi_+|^2+|\psi_-|^2$ is the total polariton concentration, and $S_z=(|\psi_+|^2-|\psi_-|^2)/2$ is the z component of the spin of the polariton condensate. $\tilde{F}$ is the exchange component of the free energy density given by

$$\tilde{F} = n_M k_B T\left[\ln Z_J\left(\frac{g_M\mu_B B_{eff}}{k_B T}\right) - \ln Z_J\left(\frac{g_M\mu_B B_0}{k_B T}\right)\right], \quad (2)$$

where n_M is the 2D concentration of magnetic ions, g_M is their g factor, μ_B is the Bohr magneton, J is the total spin of a magnetic ion (we shall assume $J=5/2$ as for $Cd_{1-x}Mn_xTe$), and T is the temperature of the system. The partition function of a magnetic ion is $Z_J(x)=\Sigma_{j=-J}^{j=+J} e^{jx}$. The total effective magnetic field acting on the magnetic ion can be represented as the sum of the real magnetic field $B_0 \geq 0$ and an effective field provoked by the spin polarization of the condensate,

$$B_{eff}(\mathbf{r}) = B_0 + \tfrac{1}{2}\lambda_M(|\psi_+|^2 - |\psi_-|^2) = B_0 + \lambda_M S_z, \quad (3)$$

with λ_M being a constant characterizing the coupling between magnetic ions and the polariton field. We neglect the Zeeman splitting of bare cavity polaritons as the corresponding g factor is usually small compared to the giant g factor induced by the exchange coupling of excitons and magnetic ions. Furthermore, we also neglect the depletion of the condensate.

In order to find the spin state of the condensate, one needs to minimize the free energy [Eq. (1)] over the z component of the pseudospin in the range $S_z \in [-n/2; n/2]$, which yields the equation

$$2\Delta_\alpha S_z = n_M g_M \mu_B \lambda_M W_J\left(\frac{g_M\mu_B B_{eff}}{k_B T}\right). \quad (4)$$

Its solutions should be compared with values of the function F at the borders of the minimization interval, i.e., for $S_z = \pm n/2$. Here $W_J(x)=\Sigma_{j=-J}^{j=+J} je^{jx}/Z_J(x)$ is the Brillouin function, plotted in Fig. 1(a).

Depending on the value of Δ_α, Eq. (4) may have zero, one, or two solutions for S_z^2, however no more than one solution corresponds to the minimum of free energy. For Δ_α close to zero the minimum free energy is achieved at one of the borders of the interval $S_z = \pm n/2$ if $B_0 \neq 0$ or at both borders if $B_0=0$. In this regime the magnetic polaron effect dominates, which is why the condensate acquires a circular polarization. If Δ_α exceeds the value

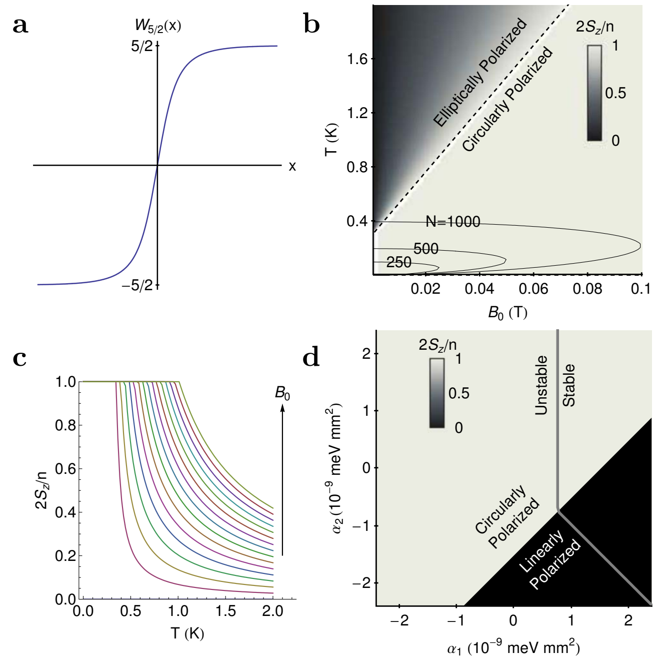

FIG. 1. (Color online) (a) The Brillouin function, $W_{5/2}(x)$. (b) Phase diagram showing the condensate circular polarization degree. The dashed line shows the boundary between circularly and elliptically polarized condensates, given by Eq. (5); solid curves show the regions of magnetic self-trapping, given by Eq. (9), for different values of N calculated for $\alpha_1=0$ (see later text). Parameters: $n_M=5\times10^{12}$ mm^{-2}, $g_M=2.02$, $\alpha_1=2.4\times10^{-9}$ meV mm^2, $\alpha_2=-0.05\alpha_1$, $\lambda_M=2.56\times10^{-11}$ T mm^2, and $n=1\times10^9$ mm^{-2}. (c) Cross sections of the circular polarization degree for fixed values of B_0. Note that for $B_0=0$ the condensate is theoretically linearly polarized, however it is unstable such that the slightest increase in magnetic field will cause a switch to a circularly polarized state. (d) Phase diagram in the (α_1,α_2) plane with $T=0.5$ K and $B_0=0$ T. Solid gray lines show the condensate stability boundary given by a change in sign of $\partial\mu/\partial n$.

$$\frac{n_M}{n} g_M\mu_B\lambda_M W_J\left(\frac{g_M\mu_B(B_0+\lambda_M n/2)}{k_B T}\right), \quad (5)$$

then the competition between the magnetic polaron effect, which favors circular polarization of the condensate, and polariton-polariton interactions, which favor its linear polarization, results in an elliptically polarized condensate $0 \leq |S_z| < n/2$. Finally, if

$$\Delta_\alpha > n_M g_M \mu_B \lambda_M \frac{\partial}{\partial S_z} W_J\left(\frac{g_M\mu_B(B_0+\lambda_M S_z)}{k_B T}\right)_{S_z\to 0}, \quad (6)$$

then the polariton-polariton interactions are so strong that no polarization of the magnetic ions due to the exchange interaction with exciton polaritons can take place and the condensate remains linearly polarized. Note that in this regime the external magnetic field would still induce some elliptical polarization of the condensate if the Zeeman effect for exciton polaritons is taken into account.[6,7] Figures 1(b)–1(d) show the polarization of the exciton-polariton condensate calculated as a function of temperature, external magnetic field, and polariton-polariton interaction constants α_1 and α_2. We estimated the polariton-magnetic ion coupling constant λ_M as

$$\lambda_M = \frac{\beta_{ex}X^2}{\mu_B g_M L_z}, \tag{7}$$

where β_{ex} is the exchange constant, X is the excitonic Hopfield coefficient of the polariton state of interest, and L_z is the QW width. For a $Cd_{1-x}Mn_xTe$ QW, at zero exciton-photon detuning, $\beta_{ex}N_0=880$ meV, where $N_0=4/a_0^3$ is the crystal cation concentration, $a_0=0.648$ nm is the lattice constant. Taking $X^2=0.5$, $L_z=10$ nm, and $g_M=2.02$ this gives $\lambda_M=2.56\times10^{-11}$ T mm^2.

The boundary between circularly and elliptically polarized condensates is shown in Fig. 1(b) for fixed interaction constants, α_1 and α_2. For very small magnetic fields at low temperatures the condensate is circularly polarized [Fig. 1(c)] and the critical temperature for transition to an elliptical condensate increases with the magnetic field. The phase diagram in the α_1-α_2 plane is shown in Fig. 1(d); for large α_1 the condensate adjusts its polarization to linear to reduce the effect of repulsive interactions.

Once the pseudospin of the condensate is found, its chemical potential can be obtained from the condition $\partial F/\partial n=0$. When taking this derivative, one should treat S_z and n as independent variables if the solution of Eq. (4) gives $S_z\neq n/2$, i.e., the polarization of the condensate differs from circular. However, if the condensate is circularly polarized, S_z and n are not independent and for the calculation of $\partial F/\partial n=0$ one sets $S_z=n/2$ in Eq. (1). The condensate is stable if $\partial\mu/\partial n>0$, otherwise the condensate collapses: it tends to increase its local density which may lead to classical condensation in real space. For the parameters used in Fig. 1(b), the condensate is always stable, however for different values of α_1 and α_2 the condensate may be unstable. The stability boundary defined by $\partial\mu/\partial n=0$ is shown in Fig. 1(d) for $B_0=0$ T (solid gray line).

If the magnetic polaron effect is strong enough, it suppresses the Bose-Einstein condensation of exciton polaritons, which is replaced by magnetic self-trapping of polaritons in real space. To describe this effect one needs to fix the number of polaritons in the system, N, to take the kinetic energy of polaritons into account when writing the free energy and to minimize the free energy FS over the inverse area occupied by the condensate S^{-1}. Assuming a parabolic dispersion of polaritons, described by an effective mass m^*, and following a variational procedure similar to that in Ref. 10, one can find the concentration of polaritons in the condensate from

$$\frac{\hbar^2}{2m^*} = -\frac{\alpha_1 N}{2} + k_B T N n_M \frac{\partial}{\partial n}\left[\frac{1}{n}\ln Z_J\left(\frac{g_M\mu_B\left(B_0+\lambda_M\frac{n}{2}\right)}{k_BT}\right) - \frac{1}{n}\ln Z_J\left(\frac{g_M\mu_B B_0}{k_BT}\right)\right]. \tag{8}$$

The critical condition for magnetic self-trapping of the polariton condensate is given by Eq. (8) in the limit $n\to0$. In this case the equation conveniently transforms to

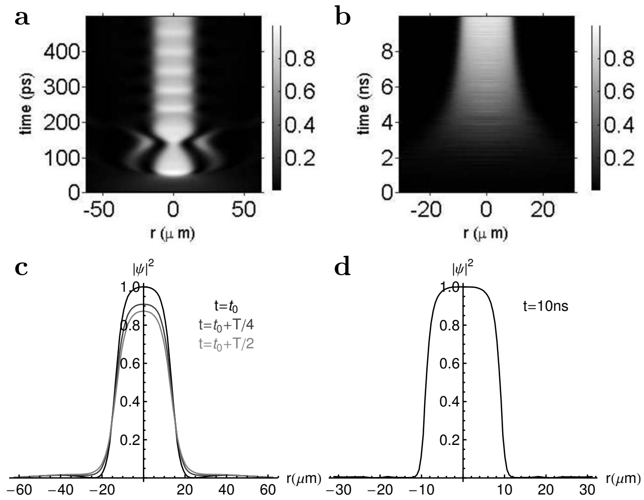

FIG. 2. Left-hand plots show the case of fast magnetic ion relaxation [$\langle M(\mathbf{r},t)\rangle=M(\mathbf{r},t)$]; right-hand plots show the case of slow magnetic ion relaxation ($\tau_M=1000$ ps). (a) and (b) show the time evolution of an initial circularly polarized Gaussian wave packet (peak intensity $|\psi|^2=n=0.5\times10^8$ mm^{-2}); the plot shows the intensity profile through a radial slice (the calculation is done in two dimensions, however the distributions are cylindrically symmetric). Parameters: $\beta=4\times10^{-18}$ meV mm^4, $B_0\sim0$, and $T=0.1$ K. Other parameters were the same as in Fig. 1. (c) Cross sections of the polariton intensity at different moments of the evolution cycle, with period $T\approx55$ ps for the case of fast magnetic ion relaxation. (d) Final intensity cross section with slow magnetic ion relaxation. $\hat{E}_{LP}$ was calculated from a two coupled oscillator model in which cavity photons and excitons had effective masses, $m_C=10^{-5}$ and $m_X=0.22$, times the free electron mass, respectively. The exciton-photon coupling energy was $V=5$ meV and there was no exciton-photon detuning.

$$\frac{\hbar^2}{m^*} = \frac{(g_M\mu_B\lambda_M)^2}{2k_BT}Nn_M \times\left[\bar{W}_J\left(\frac{g_M\mu_B B_0}{k_BT}\right) - W_J^2\left(\frac{g_M\mu_B B_0}{k_BT}\right)\right] - \alpha_1 N, \tag{9}$$

where $\bar{W}_J(x)=\Sigma_{j=-J}^{j=+J} j^2 e^{jx}/Z_J(x)$. The result of numerical solution of Eq. (9) is shown by the solid lines in Fig. 1(b) for different values of N (here we chose m^* equal to 2×10^{-5} of the free electron mass). One sees that in the absence of polariton-polariton interactions the critical temperature of magnetic polaron formation increases with increase of the occupation number of the condensate. On the other hand, repulsion between polaritons having parallel spins leads to the decrease of the critical temperature of magnetic self-trapping, which suppresses the magnetic polaron effect in microcavities. The collective magnetic polaron formation in a two-dimensional system is a second-order phase transition as the local polariton density changes continuously at the critical temperature.

In order to investigate the dynamics of classical condensation and magnetic polaron formation in real space we performed kinetic modeling using the generalized Gross-

Pitaevskii (GP) equation. Assuming no energy relaxation of the polariton condensate during its lifetime, one can write the GP equation for the condensate coupled to the magnetization relaxation equation for the magnetic medium which reads

$$i\hbar\frac{\partial\psi_\sigma}{\partial t}=\mu\psi_\sigma+\frac{\partial F}{\partial\psi_\sigma^*}=\hat{E}_{LP}\psi_\sigma-\sigma\lambda_M M\psi_\sigma + (\alpha_1|\psi_\sigma|^2+\alpha_2|\psi_{-\sigma}|^2)\psi_\sigma+\beta|\psi_\sigma|^4\psi_\sigma, \quad (10)$$

$$\frac{dM(\mathbf{r},t)}{dt}=\frac{\langle M(r,t)\rangle - M(\mathbf{r},t)}{\tau_M}, \quad (11)$$

$$\langle M(r,t)\rangle = n_M g_M \mu_B W_J\left(\frac{g_M\mu_B B_{eff}}{k_B T}\right), \quad (12)$$

$\sigma=\pm$, and τ_M is the spin relaxation time of magnetic ions. $\hat{E}_{LP}$ describes the nonparabolic dispersion of polaritons. The sextic interaction term, characterized by β (a positive constant), stabilizes the condensate during collapse.[18]

The numerical solution of Eqs. (10) and (11) can be performed using the Adams-Moulton-Bashforth method,[19] setting the initial condition to a circularly polarized Gaussian wave packet. Figures 2(a) and 2(b) show the time evolution for the case of fast and slow magnetic ion relaxations, respectively.

Absorbing boundary conditions were used to remove any radiation emitted during the transient period (a technique previously used to demonstrate soliton formation in other nonlinear Schrödinger systems[20]). In both cases the initial state evolves into a steady, spatially localized, self-trapped state when using parameters corresponding to the condensate instability. In the case of fast magnetic ion relaxation, intensity oscillations can be observed and the state is quasistable [Fig. 2(c)]; these oscillations are damped out in the case of slow magnetic ion relaxation [Fig. 2(d)]. For parameters corresponding to a stable circular or elliptic condensate the stationary solution of Eqs. (10) and (11) is always spatially homogeneous, and no bright soliton[21] propagation in real space can be observed.

In conclusion, we analyzed the effects of magnetic field and temperature on polariton condensation in dilute magnetic microcavities. We have shown that the phase diagram of the system contains regions of stable circularly and elliptically polarized condensates as well as unstable circularly polarized condensates. In the latter case polariton self-trapping in real space can occur due to the magnetic polaron effect.

We thank Yu. G. Rubo for helpful discussions and particularly for explaining that terms of sextic order should be introduced in Eq. (10) to prevent unphysical collapse of the polariton wave function. A.K. acknowledges support from EU ROBOCON and POLALAS projects.

1. S. Utsunomiya, L. Tian, G. Roumpos, C. W. Lai, N. Kumada, T. Fujisawa, M. Kuwata-Gonokami, A. Löffler, S. Höfling, A. Forchel, and Y. Yamamoto, Nat. Phys. **4**, 700 (2008).
2. A. Amo, D. Sanvitto, F. P. Laussy, D. Ballarini, E. del Valle, M. D. Martin, A. Lemaître, J. Bloch, D. N. Krizhanovskii, M. S. Skolnick, C. Tejedor, and L. Viña, Nature (London) **457**, 291 (2009).
3. F. P. Laussy, I. A. Shelykh, G. Malpuech, and A. Kavokin, Phys. Rev. B **73**, 035315 (2006); I. A. Shelykh, Yu. G. Rubo, G. Malpuech, D. D. Solnyshkov, and A. Kavokin, Phys. Rev. Lett. **97**, 066402 (2006).
4. J. Kasprzak, R. André, Le Si Dang, I. A. Shelykh, A. V. Kavokin, Yu. G. Rubo, K. V. Kavokin, and G. Malpuech, Phys. Rev. B **75**, 045326 (2007).
5. Ł. Klopotowski, M. D. Martín, A. Amo, L. Viña, I. A. Shelykh, M. M. Glazov, G. Malpuech, A. V. Kavokin, and R. André, Solid State Commun. **139**, 511 (2006).
6. Yu. Rubo, A. V. Kavokin, and I. A. Shelykh, Phys. Lett. A **358**, 227 (2006).
7. J. Keeling, Phys. Rev. B **78**, 205316 (2008).
8. T. Dietl and J. Spalek, Phys. Rev. Lett. **48**, 355 (1982).
9. S. M. Ryabchenko and Y. G. Semenov, Zh. Eksp. Teor. Fiz. **84**, 1419 (1983) [Sov. Phys. JETP **57**, 825 (1983)].
10. A. V. Kavokin and K. V. Kavokin, Sov. Phys. Semicond. **25**, 1053 (1991); Semicond. Sci. Technol. **8**, 191 (1993).
11. A. Kavokin, B. Gil, and P. Bigenwald, Phys. Rev. B **57**, R4261 (1998).
12. F. M. Marchetti, J. Keeling, M. H. Szymańska, and P. B. Littlewood, Phys. Rev. Lett. **96**, 066405 (2006); J. Keeling, P. R. Eastham, M. H. Szymanska, and P. B. Littlewood, Phys. Rev. B **72**, 115320 (2005).
13. G. Malpuech, D. D. Solnyshkov, H. Ouerdane, M. M. Glazov, and I. Shelykh, Phys. Rev. Lett. **98**, 206402 (2007).
14. J. Kasprzak, D. D. Solnyshkov, R. André, Le Si Dang, and G. Malpuech, Phys. Rev. Lett. **101**, 146404 (2008).
15. M. Combescot and O. Betbeder-Matibet, Phys. Rev. B **74**, 125316 (2006).
16. C. Ciuti, V. Savona, C. Piermarocchi, A. Quattropani, and P. Schwendimann, Phys. Rev. B **58**, 7926 (1998).
17. The ratio α_1/α_2 has been estimated as approximately 20 by P. Renucci, T. Amand, X. Marie, P. Senellart, J. Bloch, B. Sermage, and K. V. Kavokin, Phys. Rev. B **72**, 075317 (2005).
18. L. Bergé, Phys. Rep. **303**, 259 (1998).
19. D. R. Kincaid and E. W. Cheney, *Numerical Analysis* (Brooks-Cole, Belmont, MA, 1991).
20. K. Staliunas, R. Herrero, and G. J. de Valcárcel, Phys. Rev. A **75**, 011604(R) (2007).
21. O. A. Egorov, D. V. Skryabin, A. V. Yulin, and F. Lederer, Phys. Rev. Lett. **102**, 153904 (2009).